

Early response of methanogenic archaea to H₂ as evaluated by metagenomics and metatranscriptomics

Balázs Kakuk

University of Szeged: Szegedi Tudományegyetem

Roland Wirth

University of Szeged: Szegedi Tudományegyetem

Gergely Maróti

Chemical Biological Center

Szuhaj Márk

Szegedi Tudományegyetem

Gábor Rakhely

University of Szeged: Szegedi Tudományegyetem

Krisztián Laczi

Biological Research Center

Kornél Lajos Kovács (✉ kovacs.komel@bio.u-szeged.hu)

University of Szeged: Szegedi Tudományegyetem <https://orcid.org/0000-0002-3926-0497>

Zoltán Bagi

University of Szeged: Szegedi Tudományegyetem

Research

Keywords: hydrogen, biomethane, anaerobic digestion, methanogenesis, hydrogenotrophic methanogens, metagenome, metatranscriptome, renewable energy, Power-to-Gas

Posted Date: April 2nd, 2021

DOI: <https://doi.org/10.21203/rs.3.rs-368581/v1>

License: © ⓘ This work is licensed under a Creative Commons Attribution 4.0 International License.

[Read Full License](#)

Abstract

Background.

The detailed molecular machinery of the complex microbiological cell factory of biogas/biomethane production is not fully understood. One of the main puzzling process control elements is the formation, consumption and regulatory role of hydrogen (H₂). Reduction of carbon dioxide (CO₂) by H₂ is rate limiting factor in methanogenesis, but the community intends to keep H₂ concentration low in order to maintain the redox balance of the overall system. H₂ metabolism in methanogens becomes increasingly important in the Power-to-Gas renewable energy conversion and storage technologies.

Results.

The early response of the mixed mesophilic microbial community to H₂ gas injection was investigated with the goal of uncovering the first responses of the microbial community in the CH₄ formation and CO₂ mitigation Power-to-Gas process. The overall microbial composition changes, following a 10 min H₂ injection by excessive bubbling of H₂ through the reactor, was investigated via metagenome and metatranscriptome sequencing. The overall composition and taxonomic abundance of the biogas producing anaerobic community did not change appreciably two hours after the H₂ treatment, indicating that this time period was too short to display differences in the proliferation of the members of the microbial community. There was, however, a substantial increase in the expression of genes related to hydrogenotrophic methanogenesis of certain groups of Archaea. H₂ injection also altered the metabolism of a number of microbes belonging in the kingdom Bacteria. The importance of syntrophic cross-kingdom interactions in H₂ metabolism and the effects on the related Power-to-Gas process are discussed.

Conclusion

s. External H₂ regulates the functional activity of certain Bacteria and Archaea. Mixed communities are recommended for the large scale Power-to-Gas process rather than single hydrogenotrophic methanogen strains. Fast and reproducible response from the microbial community can be exploited in turn-off and turn-on of the Power-to-Gas microbial cell factories.

Background

Anaerobic digestion (AD) of organic wastes and by-products by specialized microbial communities and the concomitant biogas production is an environmentally attractive bioenergy production technology. In the context of climate change, the generation of biogas as a renewable energy form has become popular and intensively examined over the last few decades [1].

Biogas provides environmental benefits with regard to waste treatment, pollution reduction, production of CO₂-neutral renewable energy and the improvement of economy of agricultural practices through the recycling of plant nutrients and replacing artificial fertilizers [2].

Biogas can be burnt to produce heat or combusted in gas engines for electricity generation and, after purification, it can be used in any application for which fossil fuel natural gas is utilized today [3]. AD is applicable to a wide range of waste streams derived from the agro-food industry, which is a source of vast amounts of readily degradable organic material composed mainly of complex organic molecules, as well as in liquid or solid communal waste treatments.

While the main microorganisms and mechanisms involved in the methane producing anaerobic microbial cell factories are fairly well-known, the regulation and management of the overall process is far from being fully understood [4] [5]. Despite the industrial-economic importance of the underlying microbiological events, little is known about the roles, networking interactions of the microorganisms and the regulatory mechanisms of the methane production. Therefore, the microbiological events representing the bottlenecks of the process are difficult to manage. AD demands the concerted action of a complex community of microbes, each member performing their special role in the overall degradation process [6, 7]. In the absence of terminal electron acceptors such as nitrate, oxygen or sulfate, the methanogenic conversion of organic matter is an essential feature of many ecosystems [8]. The system is also a prime candidate to understand the functional networks of complex microbiological cell factories. H₂ metabolism is one of the known rate-limiting processes in AD of organic material. H₂ conversion is performed at molecular level by the class of enzymes called hydrogenases. Several hydrogenases have been identified in methanogenic archaea. With the exception of the H₂ forming methylene tetrahydromethanopterin (H₄MPT) dehydrogenase, these enzymes belong to the superfamily of nickel-iron hydrogenases [9] (Additional file 3). The series of reactions involved in methane (CH₄) formation from H₂ and carbon-dioxide (CO₂) are initiated by the formylmethanofuran dehydrogenase. This enzyme catalyzes the formation of N-carboxymethanofuran from methanofuran and CO₂ [10]. Methanogenesis from formate involves oxidation of the substrate to produce CO₂ and a reduced electron carrier. The reaction is catalyzed by a formate dehydrogenase [11]. F₄₂₀-dependent hydrogenase reduces coenzyme F₄₂₀, the central electron carrier in methanogenic archaea. Other hydrogenases from methanogens cannot reduce F₄₂₀. Hence, it is referred to as F₄₂₀-nonreducing hydrogenase [12]. In *Methanosarcina* strains, this enzyme is membrane associated. A novel hydrogenase (Ech) was discovered in acetate-grown cells of *Ms. barkeri*, which shows sequence homologies to hydrogenases 3 and 4 of *Escherichia coli* and to the CO-induced hydrogenase from *Rhodospirillum rubrum*. The purified enzyme from *Ms. barkeri* catalyzed the H₂-dependent reduction of a 2[4Fe-4S]ferredoxin and is also able to perform the reverse reaction, namely, H₂ formation from reduced ferredoxin [9].

Hydrogenases are the components of the H⁺-translocating system in methanogens [13]. The effect of H₂ on the expression of genes coding for hydrogenases and other genes has not been systematically examined yet. The exploration of the different environmental conditions, which affect the expression of

the hydrogenases and other genes could improve our knowledge concerning molecular redox mechanisms in environmental microbiology in general. It is astonishing to note the complexity of the molecular machinery, which handles the simplest molecule, H₂.

AD is one of the most promising among the various biomass conversion processes. The regulatory roles of the H₂ levels have been recognized as a significant element in the concerted action of the complex microbial community [13, 14]. We demonstrated earlier that by the introduction of H₂-producing bacteria into a natural biogas-generating consortium appreciably increased the efficacy of biogas production both in batch fermentations and in scaled-up continuous AD [13]. One of the rate-limiting factors of AD is the actual level of H₂ in the system [15]. The presence of excessive amounts of H₂ inhibits the activity of the acetogenic bacteria that generate H₂ in the system, whereas limiting H₂ levels have an adverse effect on an important group of methane producing Archaea, the hydrogenotrophic methanogens. In natural ecosystems, a very low partial pressure of H₂ is maintained, which may be a limiting factor for the methanogenesis [8, 16]. The relationship between the acetogens and methanogens is syntrophic, supported by a process called interspecies hydrogen transfer or interspecies electron flow [17]. We have only incomplete information about the detailed mechanism of interspecies hydrogen transfer [18]. The actual H₂ concentration has been shown to determine the composition of the methanogenic community [19–21]. The expression of up to 10% of the total proteins in a hydrogenotrophic methanogen were reported to change in response to H₂ limitation [22], indicating that the H₂ availability is sensed by the methanogens and this gas has a major effect on their physiology.

The reconstruction of the genomes (metagenome assembled genomes: MAGs) of the individual members of a complex microenvironment and their subsequent functional and phylogenetic analysis is termed genome-centric metagenomics [23, 24]. Genome-centric metagenomics (referred to as MG hereafter) already yielded valuable insights into the functional organization of biogas reactors and the microbial cell factories operating within [25, 26]. Additionally, its combination with metatranscriptomics (the analysis of the whole microbial community mRNA in a microenvironment), i.e. genome-centric metatranscriptomics (referred to as MTR, hereafter) enables the examination of the gene expression of each individual MAG, has been used for the in-depth analysis of the process control, regulation and interactions among the members of these cell factories.

This study is dedicated to unveil the early response of the anaerobic mixed microbial consortium, with special emphasis on methanogens to the presence of H₂ distress. This is a realistic scenario in large scale AD plants due to local concentration gradients as well as in natural environments, e.g. in swamps or rice fields. The central challenge to be understood is the regulatory role of H₂ on CH₄ formation and the early response by the methanogens and other H₂-metabolizing microbes, which regulates and balances the fragile bioenergetic processes in AD.

Results

Fermentation

A constant value of VOA/TIC is a reliable indicator of a stable mesophilic fermentation process [27]. Each experiment started with a 20 days long start-up period in order to adapt the microbial community to the alpha-cellulose substrate. During this period the average VOA and TIC values stabilized at VOA = 1.1 g L⁻¹ and the TIC = 14 g CaCO₃ L⁻¹. Because of the relatively low substrate loading rate, the VOA/TIC ratios were moderate, which allowed balanced operations. The amount of NH₄⁺ is also an important indicator of AD process stability [28]. Theoretically, levels above 3,000 mg NH₄⁺ L⁻¹ may have a negative effect on the methanogenic archaea, which is the most sensitive group of microbes in the AD process [29]. The NH₄⁺ concentration was below 1,000 mg L⁻¹ during the whole fermentation process. The biogas productivity of the digesters was also stable: 650 mL_N biogas alpha-cellulose g⁻¹ day⁻¹ were produced with 53% of CH₄ content. The first samples for DNA and RNA analysis were taken on day 20 from the stabilized reactors. After sampling the digesters were flushed with H₂ gas from a gas cylinder for 10 min and 2 hours later the second sampling was carried out. This protocol was repeated after 2 months of reactor operation.

The reactors displayed stable operation during the course of the experiment. The daily biomethane production varied by < 10%. The H₂ injection took place on days 15 and 71 (blue dotted arrows in Additional Fig. 1).

The reactors responded with a sudden increase in daily CH₄ evolution by 20–25% at both time points, which lasted for 1–2 days (Additional Fig. 1). The CH₄ content of the biogas was 53% throughout the experimental period. Afterwards the reactors returned to their previous biomethane production levels. It is worth noting that the microbial community responded exactly the same manner to the H₂ spike 2 months apart, which indicates the robustness, reproducibility and quick response time by the microbial community. Assuming H₂ saturation of the liquid phase by the H₂ bubbling for 10 min, we estimated that more than 95% of the injected H₂ was converted to CH₄ by the community within 16–24 hours, although the amount of available dissolved H₂ decreased rapidly during the second half of the H₂ consumption phase. This is in line with the observations of Szuhaj et al [30], who found in fed-batch H₂ feeding experiments at much lower scale that the injected H₂ was completely consumed in 16–24 hours and suggests that competing H₂ consuming reactions did not interfere significantly. The H₂ injection apparently did not alter markedly the cumulative biomethane production curve, which showed a straight line throughout the experiment.

Genom-centric metagenome analysis

The aim of this study was to examine the early response of the residing microbial consortium to the sudden H₂ burst at transcriptome level of metagenome-assembled genomes (MAGs). It was anticipated that the microbial composition and the relative abundances of species did not change substantially

between the samplings, i.e. within 2 hours. This way the differences in the expression levels of the genes of the MAGs could be examined.

The extensive binning procedure yielded 84 bins. Out of these, 16 were high quality, 49 were medium and 19 were low, according to the MIMAG initiative [31]. 73 bins harbored enough single copy marker genes (SCG) for the phylogenetic tree building (center part in Fig. 1.) – the phylogenetic relationship of the remaining 11 bins could not be determined.

The taxonomic assignment of the 84 bins resulted in 7 Archaea, 61 Bacteria and 16 unclassified bins (details are compiled in Additional table 1). Archaea represented about 10% of the microbiome. Within the domain Bacteria, most bins (34) were associated with the phylum *Firmicutes*. The dominance of *Firmicutes* in biogas reactors is in accordance with previous studies [8, 25]. This can be attributed to their diverse capability in polysaccharide and oligosaccharide degradation, which is the first step in the AD of complex organic substrates [32].

The second well-represented phylum was *Bacteroidetes* (12 bins), all of them belong in the order *Bacteroidales*. Most *Bacteroidetes* produce succinic acid, acetic acid, and in some cases propionic acid, these molecules fuel the acetotrophic methanogenesis. In addition, representatives of the phyla *Synergistota*, *Spirochaetes*, *Verrucomicrobia*, *Cloacimonadota*, *Fibrobacterota*, *Caldatribacteria*, and *Chloroflexota* were identified (Additional table 2). These results are also in line with previous studies [8, 25]. A typical microbial community flourished in our biogas digesters, which indicated that the synthetic medium containing only cellulose as a carbon source proved to be a good model system for the metatranscriptomic investigations [33].

A comparison of the DNA-based omics data clearly indicated that the community compositions were very similar in all four samples (Fig. 2), respectively (Additional table 1). The overall Archaea gene abundance in N₂_MTR samples was $22.9 \pm 13.4\%$ whereas in N₂-MG or H₂-MG samples the same values were $22.5 \pm 2.4\%$, respectively. This observation corroborates that i.) all reactors worked under the same conditions maintaining the same microbial community; ii.) the microbial communities did not change perceptibly within 2 hours as expected; iii.) the observations were highly reproducible after 2 months. Nevertheless, the mRNA-based metatranscriptome analysis showed striking changes in the transcriptome-based community composition when H₂ was offered to the reactors' microbial community. Approximately two times more Archaeal genes were activated 2 hours after the H₂ injection (H₂_MTR = $45.06 \pm 4.4\%$) compared to the N₂ supplied reactors. This demonstrates a rapid response to the appearance of excess H₂ by the microbial community.

The elevation of the total number of transcribed Archaeal genes (H₂_MTR samples) was mainly attributed to representatives of the genus *Methanobacterium* (bins 35 and 51), which increased from 8.6–30% of all bins abundance. *Methanobacteria* are hydrogenotrophic methanogens. The second in contribution was the order *Methanomicrobiales*. The genera *Methanoculleus* and *Methanosarcina* both belong in this order. Overall *Methanomicrobiales* showed an increase from 2.3–13.9% upon H₂ exposure.

Remarkably, the genus *Methanosarcina* effectively ceased to express genes to near zero upon H₂ dispensation (Additional table 2). *Methanosarcina* are known to possess genes coding for all three methanogenic pathways, i.e. hydrogenotrophic, acetotrophic and methylotrophic methanogenesis (e.g. 8, 16). Members of the genus *Methanoculleus* are solely hydrogenotrophic methanogens. H₂ exposure apparently turns on the activity of the hydrogenotrophic methanogenesis in *Methanoculleus* but turns off the hydrogenotrophic pathway in *Methanosarcina*.

Changes in the expression levels in methanogenesis genes

The contig assembly and ORF prediction/annotation workflow yielded 219,353 KEGG Orthology (KO) annotated ORFs. Out of these 98,791 ORFs were binned in the refined MAGs. The remaining 120,562 ORFs were used for the community-level pathway analysis. The changes in the expression levels of the genes involved in the various methanogenesis related metabolic pathways and modules were examined according to KEGG annotation. The results indicated that the methanogenesis pathway was primarily affected as the result of H₂ injection. The upregulation of differentially expressed (DE) genes was the highest in this pathway (48) and in the associated modules (Fig. 3.). It is noteworthy that some other carbon metabolism associated pathways were also affected, such as Glycolysis/Gluconeogenesis and Propanoate metabolism, which suggest that acetogenic and acetate utilizing microbes were also affected by the specifically altered environment. H₂ is known to inhibit acetogenic microbes [34], thus their response to the H₂ addition is not surprising. The RNA polymerase pathway also changed significantly, this was due to triggered transcription machinery, which had to adapt to the demands of increased transcriptional activity as a response to the altered environment.

In the binning process 4 different binning algorithms were used and the results were further refined by DAS tools (see Methods section). Despite the binning efforts, many KEGG annotated genes remained unbinned (Additional Fig. 2). Omitting these from the downstream analysis would have distorted the pathway and statistical analyses, therefore we combined them as a group of “unbinned” genes. The refined bins are also referred to as MAGs (Metagenome Assembled Genomes) hereafter.

MAGs harboring more than five KEGG map00680 pathway genes were plotted in Fig. 4.

The two MAGs identified as belonging in the genus *Methanobacterium* (bin_35 and bin_51) and bin_6 of *Methanoculleus bourgensis* showed a very similar response (Fig. 4), most of their map00680 genes are expressed at log₂ fold change (log₂FC) higher than 2, i.e. four-times higher expression. Two additional *Methanoculleus* MAGs (bin_60 and bin_66), a low and a medium quality MAG according to CheckM, were identified but not presented in Fig. 4. Nevertheless, this indicates that a number of *Methanoculleus* strains actively participate in the power-to gas (P2G) reaction.

In the hydrogenotrophic strains, the expression level of numerous genes increased shortly after H₂ injection, which indicated that the several metabolic pathways responded to the increased H₂ concentrations. The log₂FC values of the genes ENO (phosphopyruvate hydratase, EC 4.2.1.11), COF (7,8-

didemethyl-8-hydroxy-5-deazariboflavin synthase, EC 4.3.1.32), and COM (sulfopyruvate decarboxylase, EC 4.1.1.79) were the largest in *M. bourgensis*. The ENO enzyme takes part in the biosynthesis of the Coenzyme B, which is an essential molecule in the final step of the methanogenesis. The COF enzymes are responsible for the synthesis of the other important coenzyme, the Coenzyme F₄₂₀. The COM enzyme catalyze the 3-sulfopyruvate = 2-sulfoacetaldehyde reaction, which is an intermediate step of synthesis of the third important coenzyme, the Coenzyme-M [33]. These results clearly indicated that the cells increased the synthesis of all coenzymes, which are involved in methanogenesis to support the quick conversion of H₂ and CO₂ to CH₄.

In the MAGs belonging *Methanobacterium* strains, the expression level of the enzymes MFN (tyrosine decarboxylase, EC 4.1.1.25), ADC (aspartate 1-decarboxylase, EC 4.1.1.11), FMD/FWD (formylmethanofuran dehydrogenase, EC 1.2.99.5), AKS (methanogen homocitrate synthase, EC 2.3.3.14 2.3.3), COM increased. These enzymes also play an important role in the hydrogenotroph methanogenesis pathway (Additional Fig. 3). The MFN and ADC enzymes are normally involved in the methanofuran biosynthesis pathway, when they catalyze the L-tyrosine = tyramine reaction. The FMD/FWD redox enzyme complex contains a molybdopterin cofactor and numerous [4Fe-4S] clusters in order to catalyze the reversible reaction the formyl-methanofuran synthesis from methanofuran, which is an important methanogenesis step in CO₂ conversion and the oxidation of coenzyme-M to CO₂. The reaction is endergonic and is driven by coupling the soluble CoB-CoM heterodisulfide reductase via electron bifurcation. The AKS enzyme also take part in the synthesis of Coenzyme-B.

Overall, the results indicated that the hydrogenotrophic methanogenic cells activated the majority of the key enzymes in the methanogenesis pathway to consume more effectively the additional H₂. It is important that the genes of the MCR enzymes (methyl-coenzyme M reductase, EC 2.48.4.1.) showed lower expression in all hydrogenotrophic bins. The MCR enzymes (methyl-coenzyme M reductase) catalyze the final step of the methanogenesis. One of the arguments explaining this observation was that 2 hours was perhaps not enough for redirecting this section of methanogenesis pathways. If the local substrate availability did not increase significantly, the cells did not need to increase the transcriptional activity of the MCR enzymes.

Almost all genes in *Methanosarcina honorobensis* showed decreased expression in the presence of H₂ (Fig. 4). This strain has been described as acetotrophic, which also grew on methanol, dimethylamine, trimethylamine, dimethylsulfide and acetate but not on monomethylamine, H₂/CO₂, formate, 2-propanol, 2-butanol or cyclopentanol [35]. The expression levels of MCR, ACS (acetyl-CoA decarbonylase/synthase, EC 3.1.2.1) and FAE (5,6,7,8-tetrahydromethanopterin hydro-lyase, EC 4.2.1.147) significantly decreased. The ACS enzyme is responsible for the conversion of acetate to acetyl-CoA, which is a typical step in the acetotrophic methanogenesis pathway. The next enzyme, FAE generates 5,10-Methylene-THMPT from formaldehyde, an important compound, intermediate of methanogenesis.

The substantial decrease in the transcriptional response of *M. honorobensis* to H₂ injection corroborated that this strain is unable to utilize H₂, but indicated an active inhibitory role of H₂ on acetotrophic

methanogenesis. This implicates a hitherto unrecognized tight regulatory role of H₂ on diverse pathways coupled to methanogenesis (Fig. 4).

qPCR validation of the transcriptomic data

11 genes were selected for testing the metatranscriptomic data by Real-Time quantitative polymerase chain reaction (RT-qPCR). The genes were selected to cover a broad range of genes displaying various gene expression levels according to the metatranscriptomic data. Genes participating in methanogenesis as well as others involved in general in cell metabolism were included. Based on the log₂FC (Fig. 5) most of the examined genes showed consistent results with the metatranscriptomic data, although in several cases their fold change was slightly lower than derived from the metatranscriptomic analysis. Despite these minor differences, the RT-qPCR data clearly corroborated the MTR results.

Two genes, however, showed different results by RT-qPCR. The *cofG* gene had a more than 4 times smaller gene expression fold change in the qPCR experiment and it was apparently diminished into the unchanged category while the *oppA* fell from unchanged to downregulated with a two times lower fold change than in the MTR data. The latter one is a substrate-binding protein, responsible for the transport of various oligopeptides across the cell membrane [36].

Interactions between methanogenesis and other metabolic processes

In addition to the methanogenesis pathway in the archeal bins, we identified 9 additional pathways that were expressed differently as the early response of the microbiota to H₂ injection (Fig. 3B). Figure 6 presents the Archaea and Bacteria bins that indicate substantial up- or down regulation of several KEGG pathways. It is clear that H₂ addition rapidly caused gene expression changes in the Archaea, i.e. bin_6, bin_27, bin_35 and bin_51, since the Ribosome, RNA polymerase and Methanogenesis pathways were altered mainly in these bins.

In the case of Archaea, one *Methanoculleus* bin (bin_6) and the two *Methanobacteria* bins (bin_35 and bin_51) responded with elevated gene expression in all pathways, while the *Methanosarcina* (bin_27) and *Iainarchaeaia* (bin_18) responded with a substantial and general loss of transcripts, i.e. biological activity, in them.

Interestingly, the three *Methanoculleus* bins responded differently to the H₂ injection. Apparently, the entire metabolic activity, including all KEGG orthologs, were tuned up in bin_6 (classified as *M. bourgensis*), whereas only Ribosomal activity, RNA transport and Lysine biosynthesis was strongly upregulated in bin_60 and hardly any change in metabolic activity took place in bin_66 representing presumably a different strain of *M. bourgensis*. Although their overall gene expression did increase (log₂FC of 2.19 and 2.37, respectively), thus the observed differences might as well indicate a slower response by bin_60 and bin_66 and perhaps further H₂ addition would have triggered a response more similar to that of the abundant *M. bourgensis* (bin_6). If further experiments corroborate this situation, then the observation may indicate the time resolution limit of H₂ triggered transcription and metabolic

changes. It seems that the whole RNA machinery must be altered for responding to a significant change in the environment. Indeed, almost all genes (including the subunits of RNA polymerase for instance) from these pathways were highly expressed in the *Methanomicrobia* and *Methanobacteria* bins, and 64% of them with a \log_2FC of 2 or higher (p-value of 0.05 or lower). The early response to H_2 injection by *Methanosarcina horonobensis* (bin_27) was quite the opposite as the expression of all investigated KEGG orthologs and metabolic pathways were hindered significantly, i.e. up to 33% (Fig. 6).

Other carbon metabolism-related pathways that showed an overall significant difference in the pathway enrichment analysis were “carbon fixation” pathways in prokaryotes and “glycolysis / gluconeogenesis”, which showed a similar pattern. For example the *folD* gene of the reductive acetyl-CoA pathway (Wood-Ljungdahl pathway) was transcribed vigorously in bin_6 (*M. bourgensis*) ($\log_2FC = 3.7$). The relative enrichment of *Methanogenesis, acetate* \rightarrow *methane* was overall the highest in this bin (mean $\log_2FC = 3.55$), this can be linked to the elevated acetotrophic methanogenesis, as there were no other major difference between the expression change in these pathways. Interestingly though, the methanogenesis CO_2 to methane module did not increase drastically (nor did the methylotrophic module), with the exception of a handful of genes showing \log_2FC higher than 2, including methenyltetrahydromethanopterin cyclohydrolase gene in bin_6 and bin_35 ($\log_2FC = 2.56$ and 3.49 , respectively), and some others with smaller but still significant differences, including the F420-non-reducing hydrogenase iron-sulfur subunit gene of bin_6 ($\log_2FC = 1.32$, p-value = 0.04).

Changes in gene expression levels in bacterial bins

Some genes involved in, or related to elements of the methanogenesis pathway could be found in bacterial bins as well, e.g. *Herbivorax saccincola*, *Ruminiclostridium sp001512505*, two unknown *Limnochorda* and a *Mahellia* MAG. However, when inspecting the change of the methanogenesis-related KEGG orthologs in the MAGs, it becomes clear that these genes showed significant difference only in a few cases, i.e. their \log_2FC values are spread between the threshold lines that indicate significance. This means that while they are involved in the overall methanogenesis, and closely related metabolic pathways (which are included in the KEGG map00680 pathway), they did not respond to the H_2 provision change. This is substantially different from the behavior of the Archaea MAGs, which clearly express their genes differently as a response to H_2 injection.

In the case of Bacteria, the RNA-machinery pathways (ko03010) showed an overall decrease in gene expression, with the exception of bin_40 (*Treponema brennaborensis*), bin_8 (*Fermentimonas massiliensis*), bin_11 (*UBA3941_sp002385665*) and bin_7 (*Unknown Fermentimonas*). These MAGs had low abundance, though they showed an increase in the MTR samples. These pathways seem to be up-regulated in bin_40 and in bin_11 (mapped in class *Mahellia*, order *Caldicoprobaetales*). Most of the small and large ribosomal subunits showed \log_2FC of 2 or higher. Another member of the family *Treponemataceae* (bin_28 *Spiro-10 sp001604405*) showed a clear downregulation in all discussed pathways.

In AD, *Treponema* behave like the homoacetogenes, they consume H₂ and CO₂ to produce acetate, hence they may compete with hydrogenotrophic methanogens [37], although not very efficiently [16]. We identified only two methanogenesis related genes in bin_28 and bin_40 (formate-tetrahydrofolate ligase and methylenetetrahydrofolate reductase NADPH), bin_40 showed an overall activity increase (log₂FC = 2.216), indicating either that this pathway would become more active at a later time-point, or these bacteria utilize alternative catabolic activities. In a relevant observation *Treponema* abundance increased in digesters spiked with H₂ [38], although after 90 hr the signs of H₂ stress were noted in the digester. Essential genes of the Wood-Ljungdahl (WL) pathway were apparently not expressed in bacterial bins in a recent study [39]. In contrast, in the present work we identified several bins harboring these genes, including bin_7 (*Unknown Fermentimonas*), bin_8 (*Fermentimonas massiliensis*) and bin_20 (*DTU074 sp002385885*, although all of them showed low abundance (~ 0.3-1%). Interestingly, bin_20 exhibited an overall decrease, but the expression of its WL pathway genes increased. This can be attributed to the elevation of the transcriptional activity of only two genes, the *fhs* gene (formate-tetrahydrofolate ligase) and the *folD* gene (methylene-tetrahydrofolate oxidase), which are important in WL pathway (log₂FC = 6.31 and 3.14, respectively). This response to H₂ is thus the opposite to that of bin_40, suggesting that as acetogenic methanogenesis increased, it might have tried to compete with the Archaea for the acetate. The other two potential homoacetogenes, which increased their transcriptional activity (log₂FC = 1.40 and 2.56, respectively), apparently included the *fhs* and *folD* genes as well. It was also demonstrated earlier that homoacetogenic microbes tended to increase their activity in a H₂-fed systems [40].

Discussion

The interest in converting the fossil fuel based energy market to renewable energy carriers is growing worldwide. This is a very positive trend to avoid threatening global climate change and associated environmental catastrophes. The overwhelming majority of renewable energy production approaches employ photovoltaics and wind power today. Both of these technologies generate electricity in an intermittent fashion. The power distribution grids are designed to harmonize electricity production and consumption continuously, these grids can operate in a fluctuating mode only with substantial energy loss. Hence, technologies to balance the fluctuations are urgently needed. A very promising solution to this problem is offered by the flexible biogas technology [41]. Biogas plants have controllable energy output to buffer the fluctuations in renewable electricity production. Moreover, with a coupled technology called Power-to-Gas (P2G), Power-to-Methane (P2CH₄) or Power-to-Biomethane (P2bioCH₄), biogas reactors can efficiently convert the temporarily surplus renewable electricity to biomethane. Clean biomethane is chemically indistinguishable from the fossil natural gas, therefore can be stored and transported efficiently and inexpensively via the natural gas grids. The biotechnological route to P2bioCH₄ requires specific microbes capable of converting H₂ + CO₂ to CH₄ in a carbon neutral or negative carbon footprint process. The key potential player microbes are methanogenic Archaea, a group of rare and obscure obligate anaerobic microbes. The precise biochemical events leading to CH₄ formation are only understood in a broad sense today.

Understanding of the molecular regulation and control of the highly complex cell factory pathways of microbial communities carrying out AD, is a challenge for both basic and applied research. In this study we aimed at mapping the early response of the entire community, with particular attention to methanogens, a scenario frequently envisaged and expected in the P2bioCH₄ industry [30].

In a recent study thermophilic biogas reactors were fed with H₂, and after 18 hours and 36 days MTR analyses were carried out to unveil the involvement of the individual MAGs in the global microbiome functions [39]. The results revealed a multi-trophic role to *Methanosarcina thermophila*, although the hydrogenotrophic *Methanoculleus thermophilus* prevailed as the dominant Archaeal species in terms of relative gene expressions, at the expense of *M. thermophila*. Some community members that emerged in the later stages of methanogenesis were below the detection limit in the starting sample, i.e. *Methanobacteriaceae* spp.

The changes in the metatranscriptome of an AD community triggered by H₂ addition were studied before in thermophilic reactors, but the short-term response at mRNA-level to H₂ was not.

Mapping the early response of the microbial community via genome-centric metatranscriptomics is therefore important for understanding and managing the turn-on and turn-off steps of the P2bioCH₄ process. Genome-centric MG linked MTR investigations enables the distinction of the activity of each individual MAG and the identification of the key and most sensitive members of the community.

Our primary objective was to examine the initial response of the methanogenic archaea and other members of the consortia, and assess the genes that are the first up- or down-regulated ones by the H₂ injection. We used a custom bioinformatics workflow for the downstream analysis of the genes and pathways of each MAGs. This involved primarily the SqueezeMeta [42] pipeline, which can jointly analyze MG and MTR sequencing data, amended with a more extensive binning procedure, a subsequent pathway enrichment analysis and statistical evaluation of the log₂FC of the gene expressions of the MAGs between the H₂ and N₂ MTR samples. In order to gain higher statistical confidence in the results, we used biological duplicates separated by a two-month interval in CSTR AD reactors. The following important considerations were also adopted: 1.) The metagenomes of the samples separated by just a two-hour time-window, i.e. before H₂ addition and 2 hours later, to reveal whether the community composition did change in 2 hours. No perceivable changes occurred in the AD community, therefore the observed variations in the metatranscriptome were not biased by the changes in the metagenome. 2.) qPCR tests of a handful of selected genes validated the results from the metatranscriptomics pipeline. 3.)

First we established that the composition of the microbial community did not change significantly (Fig. 2), therefore the different reproduction rates of the various taxa did not disturb the picture of early functional response. Up-to-date metagenomic and metatranscriptomic methods were employed to determine the biochemical events taking place as the result of H₂ administration. The reproducibility of the system was tested by repeated H₂ injections 2 months apart. Practically identical results were obtained (Fig. 2).

Four metagenome (MG) sequencing datasets were combined to assemble a fairly large number of bins (84 bins: 7 Archaea, 61 Bacteria and 16 unclassified bins). The non-H₂-adapted, “raw” biogas forming microbial community was essentially the same in structure and composition as the ones sampled previously from the same industrial biogas plant fed with manure and maize silage [44, 45]. This community switched to H₂ consumption and biomethane production almost immediately following H₂ injection, although feeding of the entire community with alpha-cellulose substrate continued as before. We interpret that this behavior indicated the presence of sufficient hydrogenotrophic methanogenesis activity in the “raw” biogas community, i.e. in the large scale biogas plant effluent, to perform the P2bioCH₄ conversion at full speed. In other words, the diverse, “raw” anaerobic communities can be used in switching on P2bioCH₄ without a lengthy adaptation and enrichment period. This allows a quick and efficient turn-on and turn-off response by the mixed methanogenic community. The microbial community composition rearranges upon long-term exposure to H₂ (and CO₂), particularly when no other organic substrate is available for the community [45]. The vigorous P2bioCH₄ activity returned to normal biogas production as soon as the dissolved H₂ diminished, but the community was ready to adjust its biochemistry to instant H₂ conversion and P2bioCH₄ repeatedly.

The metatranscriptomic responses to the H₂ treatments separated two months apart were very similar to each other indicating that the metabolic pathways were flexibly restored after switching on and off the P2bioCH₄ operational mode. A thorough analysis of the differences between the H₂-treated metatranscriptomes and corresponding controls identified the early events in the microbial communities brought about by H₂.

H₂ (and dissolved CO₂) is readily converted to CH₄ by both direct (hydrogenotrophic) and indirect (homoacetogenesis and subsequent acetotrophic) methanogenesis. Our results suggest that the second route is unlikely the predominant one in the early response of the microbial community to H₂ addition at least under mesophilic conditions, since the acetotrophic pathways reacted sluggishly, while the gene transcription of the hydrogenotrophic route increased dramatically after a very short period of extensive H₂ feeding (Figs. 4 and 5). This predicts that under the P2bioCH₄ operation conditions the physiological readiness of the hydrogenotrophic methanogen members of the community will determine the reactor response rate upon switch-on of the H₂ addition.

Interestingly, this study revealed an extensive reaction to the transient H₂ stress within the Bacteria community as well although Bacteria cannot directly generate CH₄ from H₂ as many Archaea do. Many of these Bacteria possess the complete or partial enzyme sets for the Wood-Ljungdahl pathway. These and the homoacetogens are probably the best candidates for syntrophic community interactions between members of the distinct kingdoms of Archaea and Bacteria. The details of these interactions in the complex anaerobic environment and consequences to stabilize robust and vigorous P2bioCH₄ microbial communities during long term P2G operation should be the subjects of future studies. Nevertheless, the transcriptional activity of the primary potential syntrophic bacterial partners (bin_1 (*Herbivorax*

saccincola), bin_68 (*Ruminococcus sp.*), and unidentified bins_59, _61, _63, see Fig. 4) did not change substantially upon H₂ exposure. This may mean that either there is enough syntrophic capacity already in the non-adapted, “raw” community to support increased hydrogenotrophic methanogen activity or the syntrophic partners respond slowly to the sudden H₂ burst appearing in the microbial environment.

The development of a stable P2CH₄ community strongly depends on environmental conditions and on the starter microbial community composition. Various reactor designs, operational parameters and inocula are being tested making rigorous comparison of the results difficult.

In a brief review to summarize *in situ* biogas upgrading Zhang et al. [46], pointed out the predominant roles of the genus *Methanoculleus* under mesophilic conditions and the thermophilic genus *Methanothermobacter* at elevated temperatures. The species *M. bourgensis* (bin_6) was identified to play an important role in various biogas reactor systems. *Methanoculleus* species grow on carbon dioxide (CO₂) and hydrogen (H₂) and hence perform the hydrogenotrophic pathway for CH₄ synthesis [47]. In line with these conclusions, the mesophilic AD methanogenic community of palm oil mill effluent with eventual addition of formate was predominated by members of the genus *Methanoculleus* [48]. In a related study, various inocula were compared for biomethane production at mesophilic conditions in batch fermentations. It was concluded that the abundance and activity of the genera *Methanosarcina* and *Methanoculleus* played key roles in methanogenesis of added H₂ [48], while the authors also noted the regulatory role of the available CO₂/bicarbonate in the production of CH₄ and/or volatile fatty acids.

In a recent work [49] the microbial community changes were followed under various operational conditions starting from two distinct inocula, i.e. wastewater (WW) sludge and plug-flow reactor operated with agricultural waste (PF). The study pointed out the importance of the history of the inoculum communities. In the WW inoculated batch reactors the methanogenic genus *Methanobacterium* and *Methanothermobacter* predominated although upon H₂ feeding the genus *Methanobacterium* took over. In the plug-flow reactor, supplied with animal manure and ensilaged plant biomass, the initial abundance of genus *Methanothermobacter* diminished and the methanogenic gap was filled in by members of the genera *Methanobacterium* and *Methanoculleus*. This study corroborated the previous observations (30, 19) concerning the regulatory role of H₂ concentration and CO₂ depletion in the selection of hydrogenotrophic methanogens predominating the P2bioCH₄ community.

In a thorough *in situ* syngas bioconversion study running two UASB reactors in sequence at mesophilic temperature [50], observed the predominance of the genus *Methanothermobacter* (formerly *Methanosaeta*). The reactors were continuously fed with varying glucose loads. *Methanothermobacter* species apparently cannot carry out hydrogenotrophic methanogenesis, therefore their predominance under these conditions can be rationalized by the combined effects of glucose and CO-rich syngas addition via carboxydrotrophic methanogenesis [51]. In addition, the recently recognized capability of *Methanothermobacter* species to carry out direct electron transfer (DIET) to drive CO₂ reduction could facilitate the *Methanothermobacter* predominance [52, 53].

Taking into account these recent results and considerations, the development of a stable P2bioCH₄ mixed AD community depends on a number of important parameters, such as the origin of inoculum, H₂ supply and its fluctuation, composition of added growth supporting substrates, the dissolved CO₂/HCO₃⁻ concentration, temperature and reactor configuration.

Conclusion

In this study the early response of the mixed biogas microbial community to the presence of saturating amount of H₂ was examined. Metagenomic and metatranscriptomic analyses have been carried out to determine the changes of the expression levels of the different genes take part in the methanogenesis. The results indicated that the microbial community responded instantaneously to the presence of H₂. The activity of acetotrophs reduced significantly. In addition, the metabolic activity of numerous bacterial strains changed substantially as a response to H₂. Clearly, the excess H₂ does not only affect the methanogenesis pathways in Archaea, rather the microbial community respond with a complete gene expression profile change, which seems to be rather selective. This indicates a more global regulatory role of H₂ in the life of anaerobic communities than assumed earlier. The syntrophic interactions contribute to the stability and metabolic activity of the hydrogenotrophic methanogens. This, together with the non-sterile operation conditions and continuous supply of inexpensive catalyst, underlines the benefits of using mixed communities in the P2bioCH₄ process instead of pure hydrogenotroph cultures [30, 54, 55].

Materials And Methods

Anaerobic fermentation

Anaerobic digestions (AD) were carried out in continuously stirred tank reactors [56]. The fermentation volume was 5,000 mL, leaving a headspace of 2,000 mL. The apparatus can be fed continuously or intermittently via a piston type delivery system, the fermentation effluent is removed through an air-tight overflow. The reactors are equipped with a spiral strip mixing device driven by an electronic engine. An electronically heated jacket surrounds the cylindrical stainless steel body, electrodes for the measurement of pH and redox potential are inserted through the reactor wall, in sealed sockets. The device can be drained at the bottom. The evolved gas leaves the reactor through the top plate, where ports for gas sampling and the delivery of liquids by means of syringes through silicone rubber septa are also installed. Gas volumes are measured with thermal mass flow devices (DMFC SLA5860S, Brooks). A fresh sample from an industrial scale mesophilic biogas plant, fed with pig slurry and maize silage mix (Zöldforrás Biogas Plant, Szeged, Hungary) was used as an inoculum, i.e. the microbial community adopted to heterogeneous substrate degradation. The reactors were flushed with N₂ to ensure anaerobic conditions and were closed air tight. During the experiment the digesters were fed twice a day with synthetic medium in which only alpha-cellulose was added as a carbon source at a loading rate of 1 g oDM L⁻¹ day⁻¹. The reactors operated under mesophilic conditions, at 37°C.

Determination of fermentation parameters

Organic dry matter (oDM): The dry matter content was determined by drying the biomass at 105°C overnight and weighing the residue. Further, heating of this residue at 550°C provided the organic total solids content.

NH₄⁺-N: For the determination of NH₄⁺-N content, the Spectroquant Ammonium test (1.00683.0001 test, Merck, Kenilworth, N.J., USA) was used in a Nova 60 spectrophotometer according to the manufacturer's instructions.

VOA/TIC (Volatile organic acids/Total inorganic carbon): 5 g of each AD samples were taken for analysis and diluted appropriately with distilled water. The subsequent process was carried out with a Pronova FOS/TAC 2000 Version 812-09.2008 automatic titrator (Pronova, Germany).

Sampling

The first samples were taken when the reactor operation was stabilized under N₂ in the headspace, the daily biogas production, CH₄ content and total organic acid/buffer capacity ratio were constant. 2 mL of reactor content was taken and total RNA for transcriptome analysis (sample names: N2-MTR) and DNA for metagenome analysis (sample names: N2_MG) were isolated immediately after sampling. Then the headspace of the digesters were flushed with pure H₂ gas for 10 min. The next samples were taken 2 hours after flushing the reactors with H₂ for RNA (sample names: H2_MTR) and DNA recovery (sample names: H2_MG). The headspace was then replaced with N₂ and the reactors were run under the same conditions as before. After additional 2 months the whole H₂ treatment experiment was repeated in order to test the reproducibility of the changes. At each sampling time point two biological parallels were withdrawn.

RNA isolation and cDNA synthesis

For total RNA isolation 2 mL of reactor liquid samples were withdrawn. The samples were centrifuged at 12,000 rpm for 10 minutes. RNA extractions were carried out with the Zymo Research Soil/Fecal RNA kit (R2040, Zymo Research, Irvine, CA, United States). After lysis (bead beating), the Zymo Research kit protocol was followed. The DNA contamination was removed by Thermo Scientific Rapidout™ DNA removal kit (K2981, Thermo Fisher Scientific, Waltham, MA, United States). Ribosomal RNA was depleted using the Ribo-Zero™ rRNA Removal Kit for Bacteria (Illumina, Madison, USA) according to the manufacturer's instructions. The rRNA depleted samples were purified via the RNA Clean & Concentrator Columns from Zymo Research (Irvine, USA). During this step, an additional in-column DNase I treatment was included to ensure complete removal of DNA. Subsequently, synthesis of double-stranded cDNA was conducted using the Maxima H Minus Double-Stranded cDNA Synthesis Kit from ThermoScientific (Waltham, USA). In the first-strand cDNA synthesis reaction, 2 µL of random hexamer primer were used. Final purification of the blunt-end double-stranded cDNA was carried out using SureClean Plus solution

from Bioline (Luckenwalde, Germany). The cDNA was sequenced in the same way as the total DNA. The quality of the RNA preparation was checked by agarose gel electrophoresis (data not shown).

DNA isolation:

2 mL of samples were taken from the reactors for the isolation of nucleic acids. DNA extractions were carried out using a slightly modified version of the Zymo Research Fecal DNA kit (D6010, Zymo Research, Irvine, USA). The lysis mixture contained 100 µL of 10% CTAB (cetyltrimethylammonium bromide) to improve the efficiency [57]. After lysis (bead beating was performed by Vortex Genie 2, bead size: 0.1 mm; beating time: 15 min, beating speed: max) and subsequently the Zymo Research kit protocol was followed.

The quantity of DNA was determined in a NanoDrop ND-1000 spectrophotometer (NanoDrop Technologies, Wilmington, DE, United States) and a Qubit 2.0 Fluorometer (Life Technologies, Carlsbad, CA, United States). DNA purity was tested by agarose gel electrophoresis and on an Agilent 2200 TapeStation instrument (Agilent Technologies, Santa Clara, CA, United States).

Sequencing

Paired-end libraries were prepared for the metagenome and metatranscriptome samples using the NEBNext® Ultra™ II DNA Library Prep Kit for Illumina (Cat.Num.: E7645L). Paired-end fragment reads were generated on an Illumina NextSeq sequencer using TG NextSeq® 500/550 High Output Kit v2 (300 cycles). Raw read sequences (.fastq files) are available on NCBI-SRA under the following BioProject id: PRJNA 698464

Reverse transcription coupled quantitative PCR

11 genes were selected for reverse transcription coupled quantitative PCR (RT-qPCR) based on the metatranscriptomic data. From every sample, 500 ng of RNA was transcribed into cDNA with the High Capacity cDNA Reverse Transcription Kit (Thermo Fisher Scientific, Waltham, MA, USA) according to the instructions of the manufacturer. The PCR primer oligonucleotides were synthesized by Eurofins Genomics (Eurofins Genomics, Ebersberg Germany). The primers are listed in Additional table 3. The reactions were prepared in a final volume of 25 µL with Kapa SYBR Fast Universal qPCR kit (Roche, Basel, Switzerland). The qPCR experiments were carried out on a BioRad CFX96 Touch Real-Time PCR Detection System (BioRad, Hercules, CA, USA) with the following parameters: Initial denaturation was at 95°C for 3 min then 40 cycles of 95°C for 10 sec and 60°C for 30 sec. For quantification of the gene copies, standards were prepared with every primer pair from the genomic DNA. The standards were amplified with DreamTaq DNA Polymerase in a BioRad T100 Thermal Cycler with the following parameters: Initial denaturing was at 95°C for 3 min, then 35 cycles of 95°C for 30sec, 60°C for 30sec, 72°C for 20 sec. After amplification, the PCR products were purified with Viogene PCR Advanced PCR Clean Up Miniprep System (Viogene Biotek Corp., New Taipei City, Taiwan) following the manufacturer' instructions. The PCR product concentration was measured on a Qubit4 fluorimeter (Thermo Fisher Scientific) with a Broad

Range Assay Kit. The molarity of the PCR products was calculated based on the size and concentration of the particular gene fragment. Dilution series were created from the PCR products with a factor of 10 from 1×10^9 to 1×10^1 copies/ μ L. All dilution series were measured on the same plate with their corresponding cDNA samples in the RT-qPCR experiments. The RT-qPCR runs were evaluated with CFX Maestro version: 4.1.2433.1219 (BioRad). \log_2 FC of the gene expression was calculated as for the transcriptomics data.

Bioinformatics

Quality filtering and trimming of the raw reads were carried out with FastQC. Assembly with MegaHIT, ORF prediction with prodigal and predicted gene functional annotation was carried out within the SqueezeMeta workflow [42]. For the KEGG KO annotation EggNOG database (v. 5) was used [58]. Binning of the contigs was carried out with four different binning algorithms: Metabat2 [24], Maxbin2 [59], Concoct [23] and Binsanity [60]. The result of each binning procedure was further improved with DAS tool [61] and CheckM- bin taxonomy.

The filtered reads from each sample were mapped back onto each bins with bowtie2 [62] and FeatureCounts [63] was used to calculate the gene count table by using the ORF predictions of the bins. Since we were primarily interested in pathway analysis, genes that could be annotated with a KEGG Orthology (KO) were kept [64]. For the assessment of \log_2 fold changes (\log_2 FC) between the samples the DESeq2 package was used [65], which was proven to be a correct method to infer differences between metagenomic and metatranscriptomic gene counts [66]. The following parameters were set: test = "Wald", fitType = "parametric", filterFun = ihw. Genes with a p-value > 0.05 were termed significantly different expression (DE). The subsequent downstream analysis was carried out within the R environment by using packages of the tidyverse. Phyloseq [67] to coerce bin abundances into different taxonomic levels (e.g. Class). For visualization ggpubr package were used (<https://github.com/kassambara/ggpubr>).

Differentially expressed KOs and pathways were assessed at two levels: First, counts of genes with the same KO annotation were grouped together and summed in each sample. Differentially expressed KOs between the two MTR samples were then determined with DESeq2 as described above. The resulting DE KO list was the input for Clusterprofiler R package [68] to detect differentially expressed pathways. Then counts of genes with the same KO annotation were grouped together in each sample and in each bin, since our main focus was to assess which pathways changed in the individual genome bins. Genes that did not belong to any bin were grouped together as *unbinned*. Differentially expressed KOs of every bin between the two MTR samples were then determined with DESeq2, based on L2FC and p-values. This bin-KEGGKO-sample table was also rlog-transformed (regularized logarithm transformation) with the *rlog* function of the DESeq2 package and results were subjected to a Principal Component Analysis (PCA) using the FactoMineR package.

Declarations

Availability of data and material

All the R scripts that were used to analyze the data are available upon request. Raw read sequences (.fastq files) are available on NCBI-SRA under the following BioProject id: PRJNA698464 (<https://www.ncbi.nlm.nih.gov/bioproject/PRJNA698464>).

Acknowledgments

ZB acknowledges the funding of National Research, Development and Innovation Office OTKA program, project number FK 123902. RW and GM received partial support from the Hungarian NKFIH fund projects PD132145 and FK123899. This study has been also supported by the Hungarian National Research, Development and Innovation Fund projects GINOP- 2.2.1-15-2017-00081, EFOP- 3.6.2-16-2017-00010 and 2020-1.1.2-PIACI-KFI-2020-00117. GM was also supported by the Lendület-Programme of the Hungarian Academy of Sciences (LP2020-5/2020).

Ethics approval and consent to participate

No human or animal participants, data or tissue has been involved in the study, therefore no need for ethics approval is needed.

Consent for publication

The manuscript contains no personal information data, therefore no consent is required.

Availability of data and materials

All the R scripts that were used to analyze the data are available upon request. Raw read sequences (.fastq files) are available on NCBI-SRA under the following BioProject id: PRJNA698464 (<https://www.ncbi.nlm.nih.gov/bioproject/PRJNA698464>).

Competing interest

The authors declare that they have no competing interest.

Funding

ZB has been awarded by funding of Hungarian NKFIH/OTKA program, project number FK 123902. RW and GM received partial support from the Hungarian NKFIH fund projects PD132145 and FK123899. This study has been also supported by the Hungarian National Research, Development and Innovation Fund

projects GINOP- 2.2.1-15-2017-00081, EFOP- 3.6.2-16-2017-00010 and 2020-1.1.2-PIACI-KFI-2020-00117. GM was also supported by the Lendület-Programme of the Hungarian Academy of Sciences (LP2020-5/2020).

Authors' contributions

BK and RW performed the bioinformatic analyses. GM did the sequencing and primary evaluation of data. MSz and ZB developed the interpretation and rationalization of the data. KL contributed with the qPCR experiments. GR critically read the manuscript. KLK and BZ designed and conceived the experimental protocol and compiled the manuscript together with

Acknowledgements

ZB acknowledges the funding of Hungarian NKFIH/OTKA program, project number FK 123902. RW and GM received partial support from the Hungarian NKFIH fund projects PD132145 and FK123899. This study has been also supported by the Hungarian National Research, Development and Innovation Fund projects GINOP- 2.2.1-15-2017-00081, EFOP- 3.6.2-16-2017-00010 and 2020-1.1.2-PIACI-KFI-2020-00117. GM was also supported by the Lendület-Programme of the Hungarian Academy of Sciences (LP2020-5/2020).

References

1. Maurya R, Tirkey SR, Rajapitamahuni S, Ghosh A, Mishra S. Recent advances and future prospective of biogas production. Woodhead Publ. Ser. Energy. 2019.
2. Scarlat N, Dallemand JF, Fahl F. Biogas: Developments and perspectives in Europe. *Renew Energy*. 2018;129:457–72.
3. Bagi Z, Ács N, Böjti T, Kakuk B, Rákhely G, Strang O, et al. Biomethane: The energy storage, platform chemical and greenhouse gas mitigation target. *Anaerobe*. 2017;46:13–22.
4. Goswami R, Chattopadhyay P, Shome A, Banerjee SN, Chakraborty AK, Mathew AK, et al. An overview of physico-chemical mechanisms of biogas production by microbial communities: A step towards sustainable waste management. *3 Biotech*. 2016;6:1–12.
5. Liu CM, Wachemo AC, Tong H, Shi SH, Zhang L, Yuan HR, et al. Biogas production and microbial community properties during anaerobic digestion of corn stover at different temperatures. *Bioresour Technol*. 2018;261:93–103.
6. Maus I, Koeck DE, Cibis KG, Hahnke S, Kim YS, Langer T, et al. Unraveling the microbiome of a thermophilic biogas plant by metagenome and metatranscriptome analysis complemented by characterization of bacterial and archaeal isolates. *Biotechnol Biofuels*. 2016;9:171.
7. Hassa J, Maus I, Off S, Pühler A, Scherer P, Klocke M, et al. Metagenome, metatranscriptome, and metaproteome approaches unraveled compositions and functional relationships of microbial

- communities residing in biogas plants. *Appl Microbiol Biotechnol*. 2018;102:5045–63.
8. Wirth R, Kovacs E, Martín G, Bagi Z, Rakhely G, Kovacs KL. Characterization of a biogas producing microbial community by short read next generation DNA sequencing. *Biotechnol Biofuels*. 2012;5:1–16.
 9. Deppenmeier U. The unique biochemistry of methanogenesis. *Prog Nucleic Acid Res Mol Biol*. 2002;71:223–83.
 10. Thauer RK, Kaster AK, Goenrich M, Schick M, Hiromoto T, Shima S. Hydrogenases from methanogenic archaea, nickel, a novel cofactor, and H₂ storage. *Annu Rev Biochem*. 2010;79:507–36.
 11. Wood GE, Haydock AK, Leigh JA. Function and regulation of the formate dehydrogenase genes of the methanogenic archaeon *Methanococcus maripaludis*. *J Bacteriol*. 2003;185:2548–54.
 12. Hendrickson EL, Leigh JA. Roles of coenzyme F₄₂₀-reducing hydrogenases and hydrogen- and F₄₂₀-dependent methylenetetrahydromethanopterin dehydrogenases in reduction of F₄₂₀ and production of hydrogen during methanogenesis. *J Bacteriol*. 2008;190:4818–21.
 13. Bagi Z, Ács N, Bálint B, Horváth L, Dobó K, Perei KR, et al. Biotechnological intensification of biogas production. *Appl Microbiol Biotechnol*. 2007;76:473–82.
 14. Demirel B, Scherer P. The roles of acetotrophic and hydrogenotrophic methanogens during anaerobic conversion of biomass to methane: A review. *Rev Environ Sci Biotechnol*. 2008;7:173–90.
 15. Ács N, Bagi Z, Rákhely G, Minárovics J, Nagy K, Kovács KL. Bioaugmentation of biogas production by a hydrogen-producing bacterium. *Bioresour Technol*. 2015;186:286–93.
 16. Wahid R, Mulat DG, Gaby JC, Horn SJ. Effects of H₂:CO₂ ratio and H₂ supply fluctuation on methane content and microbial community composition during in-situ biological biogas upgrading. *Biotechnol Biofuels*. 2019;12:1–15.
 17. Lovley DR. Syntrophy Goes Electric: Direct Interspecies Electron Transfer. *Annu Rev Microbiol*. 2017;71:643–64.
 18. Barua S, Dhar BR. Advances towards understanding and engineering direct interspecies electron transfer in anaerobic digestion. *Bioresour Technol*. 2017;244:698–707.
 19. Leybo AI, Netrusov AI, Conrad R. Effect of hydrogen concentration on the community structure of hydrogenotrophic methanogens studied by T-RELP analysis of 16S rRNA gene amplicons. *Microbiology [Internet]*. 2006;75:683–8. Available from: <http://doi.org/10.1134/S0026261706060105>
 20. Kougias PG, Tsapekos P, Treu L, Kostoula M, Campanaro S, Lyberatos G, et al. Biological CO₂ fixation in up-flow reactors via exogenous H₂ addition. *J Biotechnol*. 2020;319:1–7.
 21. Hendrickson EL, Kaul R, Zhou Y, Bovee D, Chapman P, Chung J, et al. Complete genome sequence of the genetically tractable hydrogenotrophic methanogen *Methanococcus maripaludis*. *J Bacteriol*. 2004;186:6956–69.

22. Xia Q, Wang T, Hendrickson EL, Lie TJ, Hackett M, Leigh JA. Quantitative proteomics of nutrient limitation in the hydrogenotrophic methanogen *Methanococcus marisaludis*. *BMC Microbiol.* 2009;9:1–10.
23. Alneberg J, Bjarnason BS, de Bruijn I, Schirmer M, Quick J, Ijaz UZ, et al. Binning metagenomic contigs by coverage and composition. *Nat Methods.* 2014;11:1144–6.
24. Papudeshi B, Haggerty JM, Doane M, Morris MM, Walsh K, Beattie DT, et al. Optimizing and evaluating the reconstruction of Metagenome-assembled microbial genomes. *BMC Genomics.* 2017;18:915.
25. Treu L, Kougias PG, Campanaro S, Bassani I, Angelidaki I. Deeper insight into the structure of the anaerobic digestion microbial community; The biogas microbiome database is expanded with 157 new genomes. *Bioresour Technol.* 2016;216:260–6.
26. Campanaro S, Treu L, Kougias PG, Luo G, Angelidaki I. Metagenomic binning reveals the functional roles of core abundant microorganisms in twelve full-scale biogas plants. *Water Res.* 2018;140:123–34.
27. McGhee T. A method for approximation of the volatile acid concentrations in anaerobic digesters. *Water Sew Work.* 1968;115:162–6.
28. Alexander Martin. Biodegradation of organic chemicals. *Environ Sci Technol.* 1985;19:106–11.
29. Yenigün O, Demirel B. Ammonia inhibition in anaerobic digestion: A review. *Process Biochem.* 2013;48:901–11.
30. Szuhaj M, Acs N, Tengolics R, Bodor A, Rakhely G, Kovacs KL, et al. Conversion of H₂ and CO₂ to CH₄ and acetate in fed-batch biogas reactors by mixed biogas community: a novel route for the power-to-gas concept. *Biotechnol Biofuels.* BioMed Central; 2016;9:102.
31. Bowers RM, Kyrpides NC, Stepanauskas R, Harmon-Smith M, Doud D, Reddy TBK, et al. Minimum information about a single amplified genome (MISAG) and a metagenome-assembled genome (MIMAG) of bacteria and archaea. *Nat Biotechnol.* 2017;35:725–31.
32. Schwörer B, Thauer RK. Activities of formylmethanofuran dehydrogenase, methylenetetrahydromethanopterin dehydrogenase, methylenetetrahydromethanopterin reductase, and heterodisulfide reductase in methanogenic bacteria. *Arch Microbiol.* 1991;155:459–65.
33. Grochowski LL, White RH. Biosynthesis of the methanogenic coenzymes. *Compr Nat Prod II Chem Biol.* 2010;7:711–48.
34. Batstone DJ, Picioreanu C, van Loosdrecht MCM. Multidimensional modelling to investigate interspecies hydrogen transfer in anaerobic biofilms. *Water Res.* 2006;40:3099–108.
35. Shimizu S, Upadhye R, Ishijima Y, Naganuma T. *Methanosarcina horonobensis* sp. nov., a methanogenic archaeon isolated from a deep subsurface miocene formation. *Int J Syst Evol Microbiol.* 2011;61:2503–7.
36. Maqbool A, Horler RSP, Muller A, Wilkinson AJ, Wilson KS, Thomas GH. The substrate-binding protein in bacterial ABC transporters: Dissecting roles in the evolution of substrate specificity. *Biochem Soc Trans.* 2015;43:1011–7.

37. Kotsyurbenko OR, Glagolev M V, Nozhevnikova AN, Conrad R. Competition between homoacetogenic bacteria and methanogenic archaea for hydrogen at low temperature. *FEMS Microbiol Ecol.* 2001;38:153–9.
38. Li L, He Q, Ma Y, Wang X, Peng X. A mesophilic anaerobic digester for treating food waste: Process stability and microbial community analysis using pyrosequencing. *Microb Cell Fact.* 2016;15:1–11.
39. Zhu X, Campanaro S, Treu L, Seshadri R, Ivanova N, Kougias PG, et al. Metabolic dependencies govern microbial syntrophies during methanogenesis in an anaerobic digestion ecosystem. *Microbiome.* 2020;8:1–14.
40. Treu L, Kougias PG, de Diego-Díaz B, Campanaro S, Bassani I, Fernández-Rodríguez J, et al. Two-year microbial adaptation during hydrogen-mediated biogas upgrading process in a serial reactor configuration. *Bioresour Technol.* 2018;264:140–7.
41. Liebetrau J, Baier U, Wall D, Murphy JD. Integration of biogas systems into the energy system. *IEA Bioenergy*; 2020.
42. Tamames J, Puente-Sánchez F. SqueezeMeta, a highly portable, fully automatic metagenomic analysis pipeline. *Front Microbiol.* 2019;
43. Franzosa EA, McIver LJ, Rahnavard G, Thompson LR, Schirmer M, Weingart G, et al. Species-level functional profiling of metagenomes and metatranscriptomes. *Nat Methods.* 2018;15:962–8.
44. Wirth R, Böjti T, Lakatos G, Maróti G, Bagi Z, Rákhely G, et al. Characterization of core microbiomes and functional profiles of mesophilic anaerobic digesters fed with *Chlorella vulgaris* green microalgae and maize silage. *Front Energy Res.* 2019;7:1–18.
45. Ács N, Szuhaj M, Wirth R, Bagi Z, Maróti G, Rákhely G, et al. Microbial Community Rearrangements in Power-to-Biomethane Reactors Employing Mesophilic Biogas Digestate. *Front Energy Res.* 2019;7:1–15.
46. Zhang L, Kuroki A, Tong YW. A Mini-Review on In situ Biogas Upgrading Technologies via Enhanced Hydrogenotrophic Methanogenesis to Improve the Quality of Biogas From Anaerobic Digesters. *Front Energy Res.* 2020;8:1–7.
47. Maus I, Wibberg D, Stantscheff R, Stolze Y, Blom J, Eikmeyer FG, et al. Insights into the annotated genome sequence of *Methanoculleus bourgensis* MS2T, related to dominant methanogens in biogas-producing plants. *J Biotechnol.* 2015;201:43–53.
48. Woraruthai T, Kunno J, Pongsopon M, Yansakon K, Phoopraintra P, Chantiwas R, et al. Identification and cultivation of hydrogenotrophic methanogens from palm oil mill effluent for high methane production. *Int J Energy Res.* 2020;44:10058–70.
49. Logroño W, Popp D, Nikolausz M, Kluge P, Harms H, Kleinstüber S. Microbial Communities in Flexible Biomethanation of Hydrogen Are Functionally Resilient Upon Starvation. *Front Microbiol.* 2021;12:1–12.
50. Xu H, Wang K, Zhang X, Gong H, Xia Y, Holmes DE. Application of in-situ H₂-assisted biogas upgrading in high-rate anaerobic wastewater treatment. *Bioresour Technol.* 2020;299:122598.

51. Rafrafi Y, Laguillaumie L, Dumas C. Biological Methanation of H₂ and CO₂ with Mixed Cultures: Current Advances, Hurdles and Challenges. *Waste and Biomass Valorization*. 2020;
52. Nobu MK, Narihiro T, Mei R, Kamagata Y, Lee PKH, Lee PH, et al. Catabolism and interactions of uncultured organisms shaped by eco-thermodynamics in methanogenic bioprocesses. *Microbiome*. 2020;8:1–16.
53. Rotaru AE, Shrestha PM, Liu F, Shrestha M, Shrestha D, Embree M, et al. A new model for electron flow during anaerobic digestion: Direct interspecies electron transfer to Methanosaeta for the reduction of carbon dioxide to methane. *Energy Environ Sci*. 2014;7:408–15.
54. Bassani I, Kougias PG, Treu L, Angelidaki I. Biogas Upgrading via Hydrogenotrophic Methanogenesis in Two-Stage Continuous Stirred Tank Reactors at Mesophilic and Thermophilic Conditions. *Environ Sci Technol*. 2015;
55. Kougias PG, Treu L, Benavente DP, Boe K, Campanaro S, Angelidaki I. Ex-situ biogas upgrading and enhancement in different reactor systems. *Bioresour Technol*. 2017;225:429–37.
56. Kovács KL, Ács N, Kovács E, Wirth R, Rákhely G, Strang O, et al. Improvement of Biogas Production By Bioaugmentation. *Biomed Res Int*. 2013;2013:1–7.
57. Wirth R, Lakatos G, Böjti T, Maróti G, Bagi Z, Kis M, et al. Metagenome changes in the mesophilic biogas-producing community during fermentation of the green alga *Scenedesmus obliquus*. *J Biotechnol*. 2015;215:52–61.
58. Huerta-Cepas J, Szklarczyk D, Heller D, Hernández-Plaza A, Forslund SK, Cook H, et al. eggNOG 5.0: a hierarchical, functionally and phylogenetically annotated orthology resource based on 5090 organisms and 2502 viruses. *Nucleic Acids Res*. 2019;47:D309–14.
59. Wu Y-W, Simmons BA, Singer SW. MaxBin 2.0: an automated binning algorithm to recover genomes from multiple metagenomic datasets. *Bioinformatics*. 2016;32:605–7.
60. Graham ED, Heidelberg JF, Tully BJ. BinSanity: unsupervised clustering of environmental microbial assemblies using coverage and affinity propagation. *PeerJ*. 2017;5:e3035.
61. Sieber CMK, Probst AJ, Sharrar A, Thomas BC, Hess M, Tringe SG, et al. Recovery of genomes from metagenomes via a dereplication, aggregation and scoring strategy. *Nat Microbiol*. 2018;3:836–43.
62. Langmead B, Salzberg SL. Fast gapped-read alignment with Bowtie 2. *Nat Methods*. 2012;9:357–9.
63. Liao Y, Smyth GK, Shi W. The R package Rsubread is easier, faster, cheaper and better for alignment and quantification of RNA sequencing reads. *Nucleic Acids Res*. 2019;47:e47-.
64. Kanehisa M, Sato Y, Kawashima M, Furumichi M, Tanabe M. KEGG as a reference resource for gene and protein annotation. *Nucleic Acids Res*. 2015;44:D457–62.
65. Love MI, Huber W, Anders S. Moderated estimation of fold change and dispersion for RNA-seq data with DESeq2. *Genome Biol. BioMed Central*; 2014;15:550.
66. Jonsson V, Österlund T, Nerman O, Kristiansson E. Statistical evaluation of methods for identification of differentially abundant genes in comparative metagenomics. *BMC Genomics*. 2016;17:78.

67. McMurdie PJPPJ, Holmes S, Kindt R, Legendre P, O'Hara R, Metzker M, et al. Phyloseq: An R Package for Reproducible Interactive Analysis and Graphics of Microbiome Census Data. PLoS One. 2013;8:e61217.
68. Yu G, Wang LG, Han Y, He QY. ClusterProfiler: An R package for comparing biological themes among gene clusters. Omi A J Integr Biol. 2012;16:284–7.

Figures

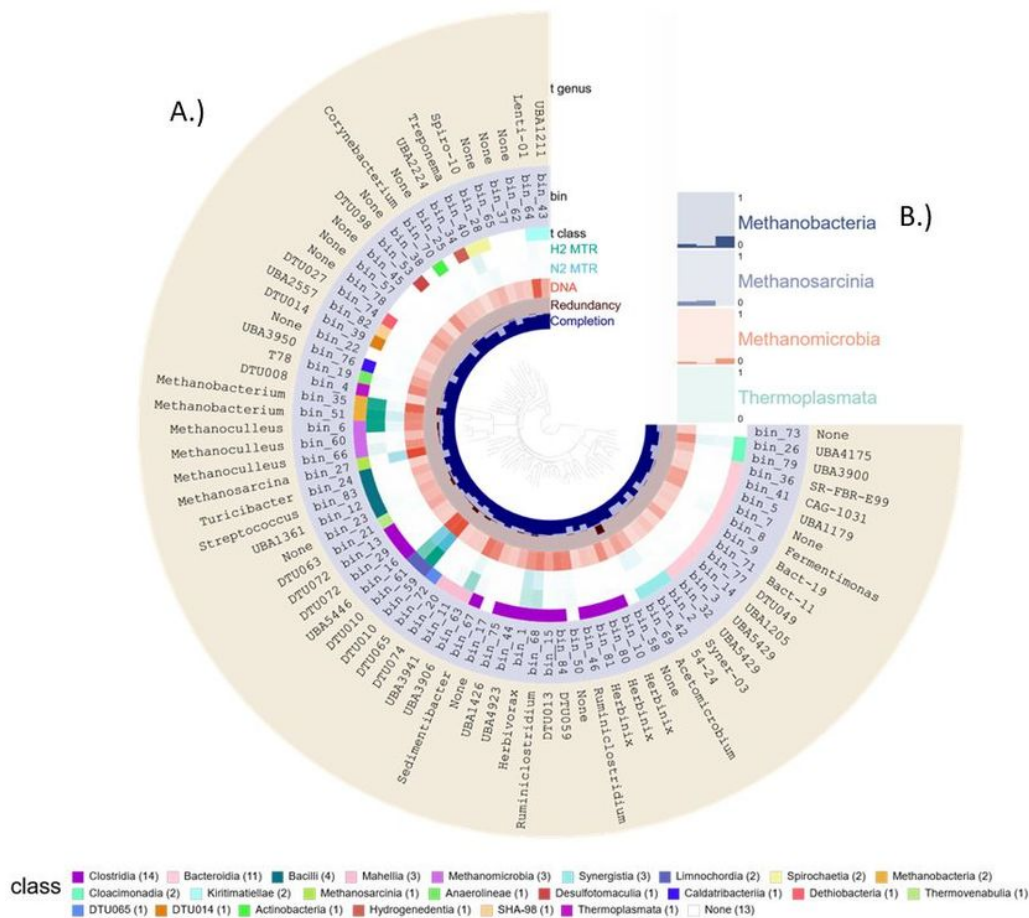


Figure 1

A.) Anvi'o plot of binning results (from innermost to outermost): phylogenetic relationship of bins according to phylophlyan3; completion and redundancy of the bins, according to single-copy marker gene (SCG) content; taxonomic Class and Genus assignment for the bins and relative abundance of bins in samples. The list of Classes at the bottom part indicates the color code and the number of bins in the Classes. B.) depicts the relative abundance of Archaeal Classes (the summary of bins in the Classes).

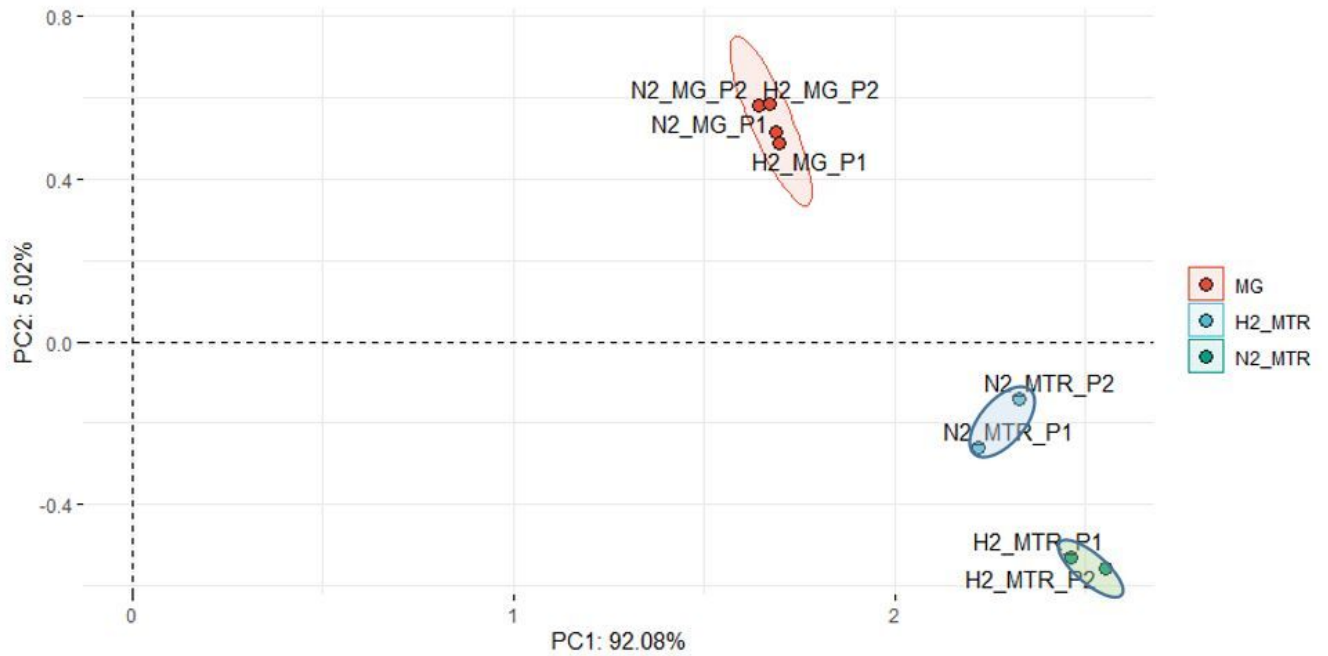


Figure 2

PCA biplot of the rlog-transformed (regularized-logarithm transformation) total gene expressions, i.e. copy number in the MG sample, of each MAG in each sample.

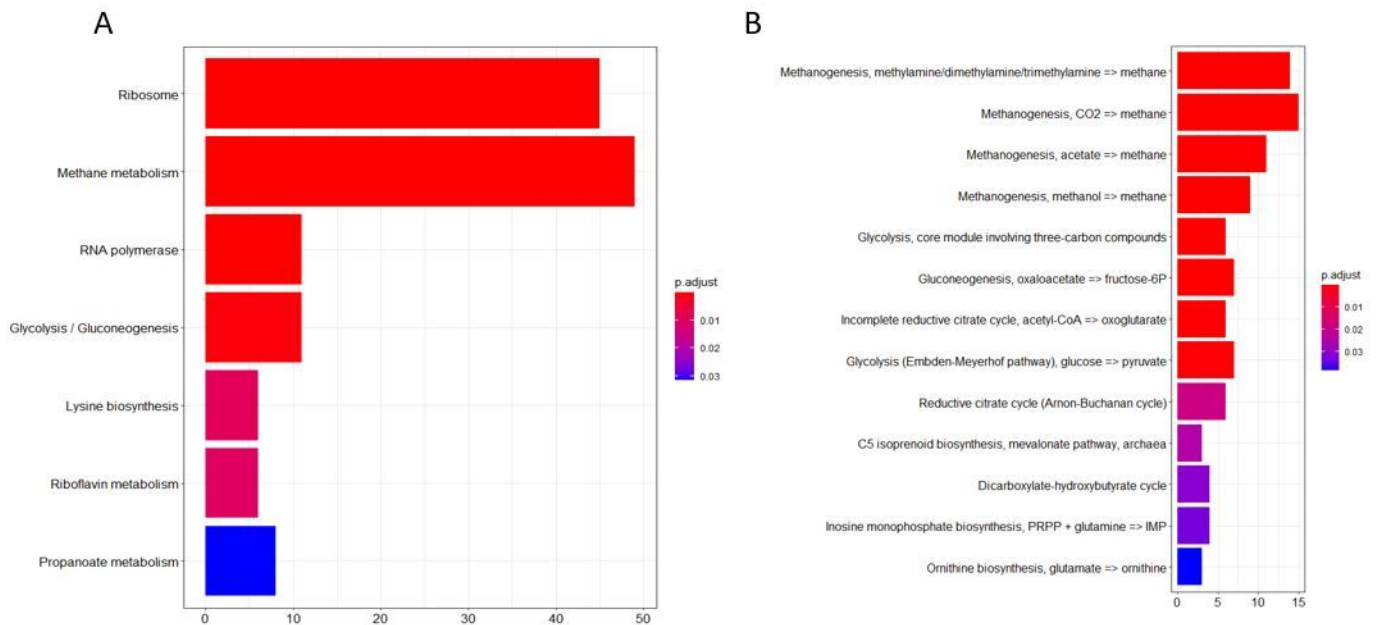


Figure 3

A.) Results of KEGG Module enrichment analysis (left), and B.) KEGG Pathway (right). The pathways, which were significantly different between N2_MTR and H2_MTR samples are presented. X-axis indicates the number of KEGG IDs found as significantly different in the given pathway (listed along the Y axis). P-adjust stands for corrected p-values.

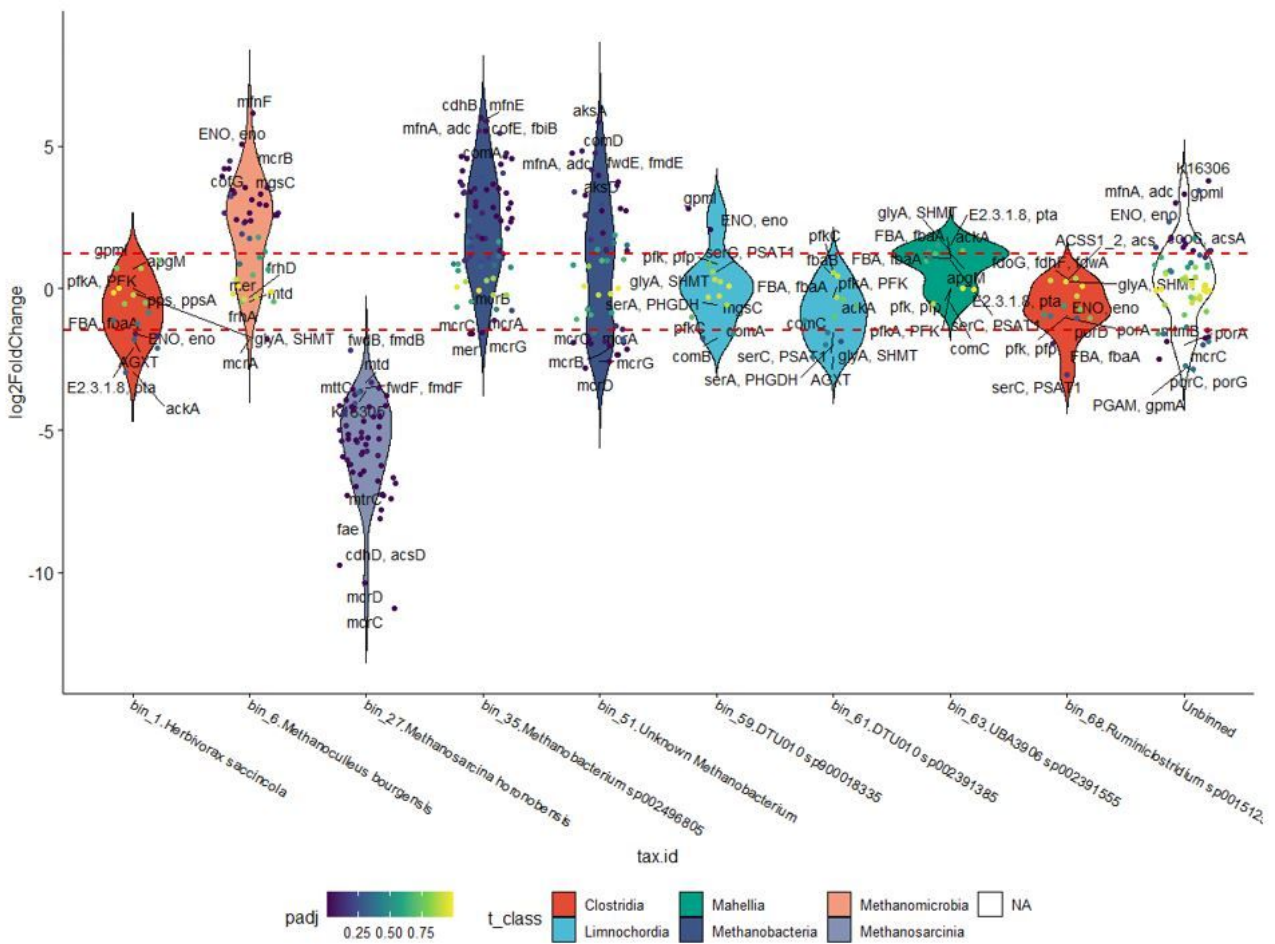


Figure 4

Violin plot of genes (small dots) involved in the methanogenesis KEGG pathway (map00680) in each bin (arranged on the X-axis) and the unbinned gene collection. Only bins, which contain at least 5 methanogenesis genes are plotted. Filling colors indicate taxonomy at Class level. Each dot represents a KEGG orthologue (KO) in the respective bin. Colors of the dots indicate the p-value of the log2FC difference between N2_MTR and H2_MTR samples. Horizontal dashed red lines mark the log2FC thresholds for significantly different KOs (respective p-value < 0.05).

Name of the encoded protein	Genes	Bin	log ₂ fold change in metatranscriptome		qPCR log ₂ fold change	
methyl-CoM reductase beta subunit	<i>mcrB</i>	bin_27		-6.24		-8.79
(4-(4-[2-(gamma-L-glutamylamino)ethyl]phenoxy)methyl)furan-2-yl)methanamine synthase	<i>mfnF</i>	bin_6		3.23		2.57
7,8-didemethyl-8-hydroxy-5-deazariboflavin synthase	<i>cofG</i>	bin_6		4.20		0.98
Ribosomal protein L10	<i>rplJ</i>	bin_6		6.48		4.77
Coenzyme F420 hydrogenase subunit alpha	<i>frhA</i>	bin_27		-4.66		-5.75
enolase	<i>eno</i>	bin_6		5.06		4.19
glyceraldehyde 3-phosphate dehydrogenase	<i>gapA</i>	bin_59		3.65		3.01
peptid nickel transport system substrate binding protein	<i>oppA</i>	bin_59		-1.45		-2.93
pyruvate, phosphate dikinase	<i>ppdK</i>	bin_1		-1.52		-1.37
acetyl-CoA decarboxylase/synthase	<i>cdhC</i>	bin_27		-6.87		-8.84
methyl-CoM reductase gamma subunit	<i>mcrC</i>	bin_35		-1.58		-1.83

Figure 5

Comparison of metatranscriptomic and qPCR results of selected genes affected by early H2 treatment.

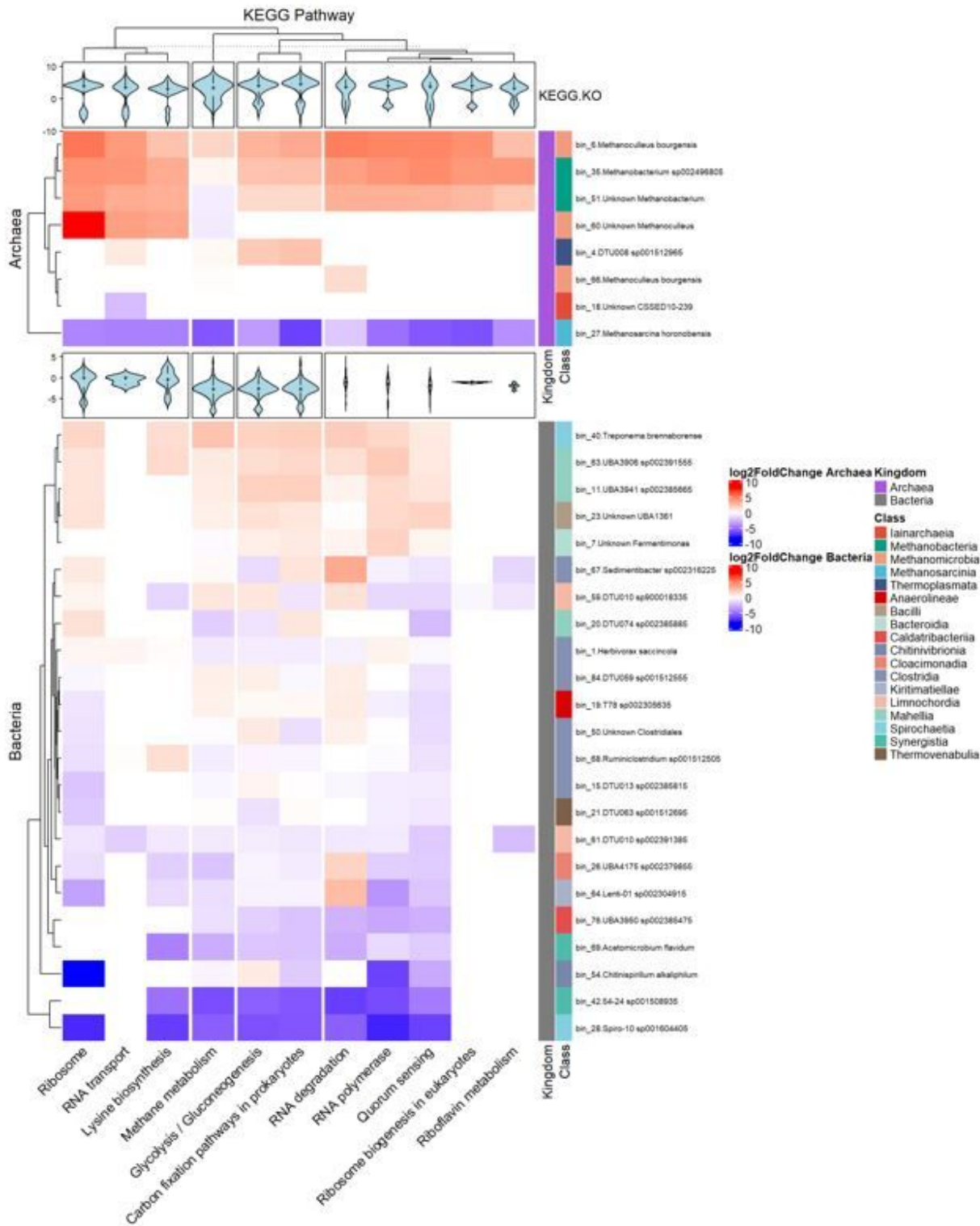


Figure 6

Heatmap of significantly various KEGG Pathways in bins that harbor a total of at least 10 genes in any of these pathways or modules. Top panel shows Archaeal, while the bottom panel shows Bacterial bins. Filling colors are according to the log₂FC of all the genes in that pathway/module in the given bin. Violin plots represent log₂FC values of every gene participating in the given pathway/module.

Supplementary Files

This is a list of supplementary files associated with this preprint. Click to download.

- [Suppl.fig.1.Biogasyields.pptx](#)
- [Suppl.fig.2Binsabundances.pptx](#)
- [Suppl.fig.3Methanogenesisenzymes.pptx](#)
- [Supplementarytable1Sequencinginfo.xlsx](#)
- [Supplementarytable2MAGsinfo1.xlsx](#)
- [Supplementarytable3qPCRprimers.pptx](#)